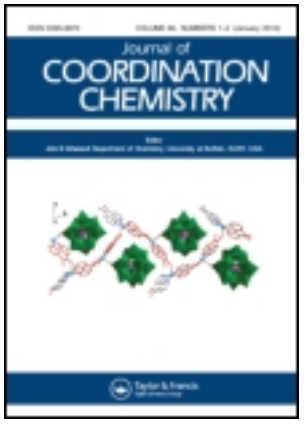

Journal of Coordination Chemistry
Publication details, including instructions for authors and subscription information:
http://www.tandfonline.com/loi/gcoo20

DNA-binding and anti-oxidation properties of binuclear lanthanide(III) complexes of 8-hydroxyquinoline-7-carbaldehyde-(isonicotinyl)hydrazone

Yongchun Liu [a], Kejun Zhang [a], Ruixia Lei [a], Jianning Liu [a], Tianlin Zhou [a] & Zheng-Yin Yang [b]

[a] Key Laboratory of Longdong Biological Resources in Gansu Province, College of Chemistry and Chemical Engineering, Longdong University, Gansu 745000, Qingyang, P.R. China

[b] State Key Laboratory of Applied Organic Chemistry, College of Chemistry and Chemical Engineering, Lanzhou University, Lanzhou 730000, P.R. China

Published online: 22 May 2012.

To cite this article: Yongchun Liu, Kejun Zhang, Ruixia Lei, Jianning Liu, Tianlin Zhou & Zheng-Yin Yang (2012) DNA-binding and anti-oxidation properties of binuclear lanthanide(III) complexes of 8-hydroxyquinoline-7-carbaldehyde-(isonicotinyl)hydrazone, Journal of Coordination Chemistry, 65:12, 2041-2054, DOI: 10.1080/00958972.2012.683485

To link to this article: http://dx.doi.org/10.1080/00958972.2012.683485

Journal of Coordination Chemistry
Vol. 65, No. 12, 20 June 2012, 2041–2054

DNA-binding and anti-oxidation properties of binuclear lanthanide(III) complexes of 8-hydroxyquinoline-7-carbaldehyde-(isonicotinyl)hydrazone

YONGCHUN LIU*†, KEJUN ZHANG†, RUIXIA LEI†, JIANNING LIU†, TIANLIN ZHOU† and ZHENG-YIN YANG‡

†Key Laboratory of Longdong Biological Resources in Gansu Province, College of Chemistry and Chemical Engineering, Longdong University, Gansu 745000, Qingyang, P.R. China
‡State Key Laboratory of Applied Organic Chemistry, College of Chemistry and Chemical Engineering, Lanzhou University, Lanzhou 730000, P.R. China

(*Received 27 December 2011; in final form 7 March 2012*)

Binuclear complexes $[LnL(NO_3)(H_2O)_2]_2$ were prepared from the Schiff base 8-hydroxyquinoline-7-carbaldehyde-(isonicotinyl)hydrazone (H_2L) and equivalent molar amounts of $Ln(NO_3)_3 \cdot 6H_2O$ ($Ln = La^{3+}$, Nd^{3+}, Sm^{3+}, Eu^{3+}, Gd^{3+}, Dy^{3+}, Ho^{3+}, Er^{3+}, Yb^{3+}), respectively. The ligand is dibasic tetradentate and the dimerization occurs through the phenolate oxygen atoms leading to a central four-membered $(LnO)_2$-ring. The ligand and all the Ln(III) complexes can bind to calf thymus DNA through intercalation with binding constants of 10^5–10^6 $(mol\,L^{-1})^{-1}$, and they show strong scavenging abilities on hydroxyl radicals and superoxide radicals. The values of SC_{50} of Ln(III) complexes for $HO^{\bullet}$ and $O_2^{\bullet-}$ are 2.344−13.33 and 4.459−28.48 μmol L^{-1}, respectively. Ln(III) complexes present stronger binding abilities to DNA and stronger anti-oxidation properties than ligand. Complex containing hydroxyl unit shows stronger scavenging abilities on hydroxyl radical, while complex containing *N*-heteroaromatic substituent shows stronger scavenging abilities on superoxide radicals. Furthermore, earlier rare metal complexes show stronger scavenging abilities on both hydroxyl radicals and superoxide radicals.

Keywords: 8-Hydroxyquinoline-7-carbaldehyde; Schiff-base ligand; Lanthanide(III) complexes; Calf thymus DNA; Intercalation; Anti-oxidation properties

1. Introduction

DNA is an important cellular receptor, many chemicals exert their antitumor effects through binding to DNA thereby changing the replication of DNA and inhibiting the growth of tumor cells, which is the basis for designing more efficient antitumor drugs; their effectiveness depends on the mode and affinity of the binding [1–3]. A number of metal chelates, as agents for mediation of strand scission of duplex DNA and as chemotherapeutic agents, have been used as probes of DNA structure in solution [4–6]. Apart from magnetic and photophysical properties, the bioactivities of lanthanides such

*Corresponding author. Email: ychliu001@163.com

ISSN 0095-8972 print/ISSN 1029-0389 online © 2012 Taylor & Francis
http://dx.doi.org/10.1080/00958972.2012.683485

as antimicrobial, antitumor, antivirus, anticoagulant action, enhancing NK and macrophage cell activities, and prevention from arteriosclerosis have been explored [7–10]. An excess of activated oxygen species, superoxide anion ($O_2^{-\bullet}$), and hydroxyl radical ($OH^{\bullet}$), generated by normal metabolic processes, may cause various diseases such as carcinogenesis, drug-associated toxicity, inflammation, atherogenesis, and aging in aerobic organisms [11–13]. Some minor groove binders for DNA are effective inhibitors of formation of a DNA/TBP complex or topoisomerases. Adding a reactive entity endowed with oxidative properties should improve the efficiency of inhibitors [14–16]. Well-designed organic ligands enable fine tuning of properties of the metal ions. Quinoline and its derivatives have attracted special interest due to their therapeutic properties. Quinoline sulphonamides have been used in the treatment of cancer, tuberculosis, diabetes, malaria, and convulsion for decades [17, 18].

Previously, we investigated biological properties of lanthanide(III) complexes of Schiff bases derived from 8-hydroxyquinoline-2-carbaldehyde with some aroylhydrazines and 8-hydroxyquinoline-7-carbaldehyde with benzoylhydrazine. All these ligands and rare-earth metal complexes showed strong anti-oxidation and DNA-binding properties, useful as potential anticancer drugs [19–24]. In this article, the Schiff base derived from 8-hydroxyquinoline-7-carbaldehyde with isonicotinylhydrazine and its lanthanide(III) complexes are prepared to investigate their anti-oxidation and DNA-binding properties.

2. Experimental

2.1. *Materials*

Calf thymus DNA (ct-DNA) and ethidium bromide (EB) were obtained from Sigma-Aldrich Biotech. Co., Ltd. Stock solution (1.0 mmol L^{-1}) of the investigated compound was prepared by dissolving the powdered material into appropriate amounts of DMF. Deionized double distilled water and analytical grade reagents were used throughout. ct-DNA stock solution was prepared by dissolving the solid material in 5 mmol L^{-1} Tris-HCl buffer (pH 7.20) containing 50 mmolL^{-1} NaCl. The ct-DNA concentration in terms of base pair L^{-1} was determined spectrophotometrically by employing an extinction coefficient of $\epsilon = 13{,}200\,(\text{mol L}^{-1})^{-1}\,\text{cm}^{-1}$ (base pair)$^{-1}$ at 260 nm and the concentration in terms of nucleotide L^{-1} was also determined spectrophotometrically by employing an extinction coefficient of 6600 $(\text{mol L}^{-1})^{-1}\,\text{cm}^{-1}$ (nucleotide)$^{-1}$ at 260 nm [25]. The stock solution was stored at −20°C until it was used. EB was dissolved in 5 mmol L^{-1} Tris-HCl buffer (pH 7.20) containing 50 mmol L^{-1} NaCl and its concentration was determined assuming a molar extinction coefficient of 5600 L $\text{mol}^{-1}\,\text{cm}^{-1}$ at 480 nm [26].

2.2. *Methods*

Melting points of the compounds were determined on an XT4-100X microscopic melting point apparatus (Beijing). Elemental analyses of C, N, and H were carried out on an Elemental Vario EL analyzer. The metal ion content was determined by complexometric titration with EDTA after destruction of the complex in the

conventional manner. Infrared (IR) spectra were recorded on a Nicolet Nexus 670 FT-IR spectrometer using KBr discs from 4000 cm^{-1} to 400 cm^{-1}. ^1H NMR spectra were recorded on a Bruker Advance DRX 200-MHz spectrometer with tetramethylsilane (TMS) as an internal standard. ESI-MS (ESI-Trap/Mass) spectra were recorded on a Bruker Esquire6000 Mass spectrophotometer and formic acid was used as the proton source.

Viscosity titration experiments were carried on an Ubbelohde viscometer in a thermostated water-bath maintained at $25.00 \pm 0.01^{\circ}C$. Data were presented as $(\eta/\eta_o)^{1/3}$ *versus* the ratio of the compound to DNA, where η is the viscosity of DNA in the presence of the compound corrected from the solvent effect and η_o is the viscosity of DNA alone [26, 27].

Ultraviolet-Visible (UV-Vis) spectra were obtained using a Perkin Elmer Lambda UV-Vis spectrophotometer. The binding constant (K_b) was determined by the following equation [28, 29]:

$$\frac{[DNA]}{\varepsilon_f - \varepsilon_a} = \frac{[DNA]}{\varepsilon_f - \varepsilon_b} + \frac{1}{K_b(\varepsilon_f - \varepsilon_b)}, \tag{1}$$

where [DNA] is the molar concentration of DNA in base pairs, ϵ_a ($(mol\,L^{-1})^{-1}\,cm^{-1}$) corresponds to the extinction coefficient observed, ϵ_f ($(mol\,L^{-1})^{-1}\,cm^{-1}$) corresponds to the extinction coefficient of the free compound, ϵ_b ($(mol\,L^{-1})^{-1}\,cm^{-1}$) is the extinction coefficient of the compound when fully bound to DNA, and K_b is the intrinsic binding constant. The ratio of slope to intercept in the plot of $[DNA]/(\epsilon_f - \epsilon_a)$ *versus* [DNA] gives the value of K_b.

Fluorescence spectra were recorded using an RF-5301PC spectrofluorophotometer (Shimadzu, Japan) with a 1 cm quartz cell. Both excitation and emission band widths were 10 nm. DNA-EB quenching assay was performed according to literature procedure [19, 20]. DNA (4.0 $\mu mol\,L^{-1}$, nucleotides) solution was added incrementally to 0.32 $\mu mol\,L^{-1}$ EB solution, then small aliquots of concentrated solutions (1.0 $mmolL^{-1}$) were added till the drop in fluorescence intensity ($\lambda_{ex} = 525$ nm, $\lambda_{em} = 587$ nm) reached a constant value. Measurements were made after 5 min at 298 K. The Stern–Volmer equation was used to determine the fluorescence quenching mechanism [30]:

$$F_o/F = 1 + K_{SV}[Q], \tag{2}$$

where F_o and F are the fluorescence intensity in the absence and presence of a compound at [Q], respectively; K_{SV} is the Stern–Volmer dynamic quenching constant.

Hydroxyl radicals ($OH^{\bullet}$) in aqueous media were generated through the Fenton-type reaction [31, 32]. The 5 mL reaction mixtures contained 2.0 mL of 100 $mmolL^{-1}$ phosphate buffer (pH = 7.4), 1.0 mL of 0.10 $mmolL^{-1}$ aqueous safranin, 1 mL of 1.0 $mmolL^{-1}$ aqueous EDTA-Fe(II), 1 mL of 3% aqueous H_2O_2, and a series of quantitatively microadding solutions of the tested compound. The reaction mixtures were incubated at 37°C for 60 min in a water-bath. Absorbance at 520 nm was measured and the solvent effect was corrected throughout. The scavenging effect for $OH^{\bullet}$ was calculated from the following expression [33, 34]:

$$\text{Scavenging effect (\%)} = \frac{A_{sample} - A_{blank}}{A_{control} - A_{blank}} \times 100, \tag{3}$$

where A_{sample} is the absorbance of the sample in the presence of the tested compound, A_{blank} is the absorbance of the blank in the absence of the tested compound, and $A_{control}$ is the absorbance in the absence of the tested compound and EDTA-Fe(II).

Superoxide radicals ($O_2^{\bullet}$) were produced by the MET-VitB_2-NBT system [33, 34]. The 5 mL reaction mixtures contained 2.5 mL of 100 mmol L^{-1} phosphate buffer (pH 7.8), 1.0 mL of 50 mmol L^{-1} MET (methionine), 1.0 ml of 0.23 mmol L^{-1} NBT (nitroblue tetrazolium), 0.50 ml of 33 μmol L^{-1} VitB_2 (vitamin B_2), and a series of quantitatively microadding solutions of the tested compound in the absence of light. After incubation at 30°C for 10 min in a water-bath and then illumination with a fluorescent lamp (4000 Lux), the absorbance of the sample was measured at 560 nm and the solvent effect was corrected throughout. The scavenging effect for $O_2^{\bullet}$ was calculated from the following expression:

$$\text{Scavenging effect } (\%) = \frac{A_o - A_i}{A_o} \times 100, \quad (4)$$

where A_i is the absorbance in the presence of the tested compound and A_o is the absorbance in the absence of the tested compound.

Data for anti-oxidation are presented as means ±SD of three determinations and followed by Student's *t*-test. Differences were considered to be statistically significant if $p < 0.05$. SC_{50} value, calculated from the regression line of the log of the tested compound concentration *versus* the scavenging effect (%) of the compound, is introduced to denote the molar concentration of the tested compound which causes a 50% scavenging effect on hydroxyl radicals or superoxide radicals.

2.3. *Synthesis of 8-hydroxyquinoline-7-carbaldehyde*

8-Hydroxyquinoline-7-carbaldehyde was prepared as previously reported [35–37]. Chloropicrin (32 mL, 0.4 mol) was dropped into ethanol solution of 14.5 g (0.1 mol) 8-hydroxyquinoline and 40% NaOH (1 mol) aqueous solution. Refluxing the mixture at 65–70°C for 4 h, the crude product was obtained after acidification at pH 5.0−5.5 by 0.1 mol L^{-1} HCl. A salmon pink crystal was separated, obtained by chromatographic column (eluent, $V_{petroleum} : V_{ethyl\ acetate} = 40 : 1$). Then, recrystallization by chloropicrin and ethanol gave 3.1 g pale-orange needle-like crystals after drying by vacuum, yield 18%, m.p. 178°C.

2.4. *Synthesis of 8-hydroxyquinoline-7-carbaldehyde-(isonicotinyl)hydrazone (1)*

Ligand **1** (H_2L) was prepared by refluxing and stirring a mixture of 10 mL ethanol solution of 8-hydroxyquinoline-7-carbaldehyde (0.519 g, 3 mmol) and a 10 mL 90% ethanol aqueous solution of isonicotinylhydrazine (0.411 g, 3 mmol) for 8 h. After cooling to room temperature, the precipitate was filtered, recrystallized from 80% methanol aqueous solution, and dried in vacuum over 48 h to give a pale yellow powder, yield 72.3% (0.633 g); m.p. 251−252°C. UV-Vis (λ_{max} nm, $\epsilon \times 10^4$ $(mol\ L^{-1})^{-1}\ cm^{-1}$): 246 (2.17), 353 (1.57). IR (KBr): 3335, 3190, 1642, 1592, 1568, 1551, 1231. Anal. Calcd for $C_{16}H_{12}N_4O_2$ (%): C, 65.75; H, 4.14; N, 19.17. Found: C, 65.67; H, 4.12; N, 19.22. MS (ESI-TOF) *m/z*: 293.1 $[M + H]^+$. ^1H NMR (DMSO-d_6,

200 MHz, TMS) δ: 12.032 (1H, s, 13-NH), 9.619–9.586 (1H, dd, $J_{23} = 8.7$ Hz, $J_{24} = 1.2$ Hz, 2-CH), 8.964–8.947 (1H, s, 11-CH=N), 8.830–8.800 (3H, m, 4-CH, 17-CH, 19-CH), 7.872–7.853 (2H, d, $J = 5.7$ Hz, 16-CH, 20-CH), 7.825–7.800 (1 H, d, $J = 7.5$ Hz, 6-CH), 7.778–7.735 (1H, m, 3-CH), 7.194–7.169 (1H, d, $J = 7.5$ Hz, 5-CH).

2.5. *Synthesis of metal complexes (2–10)*

Each Ln(III) complex was prepared by refluxing and stirring a mixture of a 40 mL methanol solution of **1** (0.058 g, 0.2 mmol) and an equivalent molar amount of $Ln(NO_3)_3 \cdot 6H_2O$ ($Ln = La^{3+}$, Nd^{3+}, Sm^{3+}, Eu^{3+}, Gd^{3+}, Dy^{3+}, Ho^{3+}, Er^{3+}, Yb^{3+}) on a water-bath, respectively. After refluxing for 30 min, triethylamine (0.020 g, 0.2 mmol) was added dropwise to deprotonate the phenolic hydroxyl substituent of 8-hydroxyquinolinate. Then, the mixture was refluxed and stirred continuously for 8 h. Cooling to room temperature, the precipitate was centrifuged, washed with methanol, and dried in vacuum over 48 h to give a powder. All the Ln(III) complexes are yellow powders and their melting points exceed 300°C.

Complex **2**: Yield 89.7% (0.095 g). UV-Vis (λ_{max} nm, $\epsilon \times 10^4$ $(mol\,L^{-1})^{-1}\,cm^{-1}$): 248 (4.63), 356 (3.26). IR (KBr): 3390, 3206, 1654, 1591, 1555, 1096, 1465, 1319, 1034, 965, 839, 721, 634, 533, 436. MS (ESI-TOP, DMF) *m/z*: 293.1, 636.5, 637.4, 638.1, 638.6, 639.3, 1273.0, 1275.1, 1277.3. Anal. Calcd for $C_{32}H_{28}N_{10}O_{14}La_2$ (%): C, 36.45; H, 2.68; N, 13.28; La, 26.35. Found: C, 36.72; H, 2.65; N, 13.19; La, 26.44. Λm ($cm^2\,\Omega^{-1}\,mol^{-1}$, DMF): 51.1.

Complex **3**: Yield 87.8% (0.094 g). UV-Vis (λ_{max} nm, $\epsilon \times 10^4$ $(mol\,L^{-1})^{-1}\,cm^{-1}$): 248 (4.68), 356 (3.52). IR (KBr): 3369, 3215, 1655, 1590, 1557, 1095, 1465, 1318, 1046, 965, 839, 725, 631, 534, 442. MS (ESI-TOP, DMF) *m/z*: 293.2, 640.1, 640.4, 640.9, 641.3, 643.3, 643.6, 644.0, 644.3, 644.7, 646.1, 647.0, 647.6, 648.0, 648.8, 649.5, 650.2, 1280.5, 1281.2, 1281.8, 1282.7, 1283.3, 1284.8, 1285.6, 1286.3, 1287.5, 1288.4, 1289.9, 1290.4, 1291.3, 1291.7, 1293.3, 1294.0, 1294.9, 1295.4, 1296.1, 1296.5, 1297.7, 1299.0, 1299.8. Anal. Calcd $C_{32}H_{28}N_{10}O_{14}Nd_2$ (%): C, 36.08; H, 2.65; N, 13.13; Nd, 27.08. Found: C, 36.13; H, 2.65; N, 13.24; Nd, 27.01. Λm ($cm^2\,\Omega^{-1}\,mol^{-1}$, DMF): 45.3.

Complex **4**: Yield 87.2% (0.094 g). UV-Vis (λ_{max} nm, $\epsilon \times 10^4$ $(mol\,L^{-1})^{-1}\,cm^{-1}$): 262 (4.01), 365 (2.40), 393 (2.38). IR (KBr): 3376, 3216, 1655, 1591, 1558, 1097, 1467, 1323, 1031, 965, 840, 726, 634, 535, 442. MS (ESI-TOP, DMF) *m/z*: 293.1, 642.1, 643.1, 644.4, 645.1, 646.0, 647.2, 647.6, 648.1, 648.6, 649.2, 650.2, 650.8, 651.3, 651.8, 653.6, 654.1, 1284.9, 1288.4, 1289.1, 1291.1, 1293.4, 1294.7, 1297.7, 1300.3, 1301.0, 1304.3, 1305.1, 1306.2. Anal. Calcd for $C_{32}H_{28}N_{10}O_{14}Sm_2$ (%): C, 37.97; H, 2.81; N, 10.42; Sm, 27.96. Found: C, 38.13; H, 2.80; N, 10.37; Sm, 27.81. Λm ($cm^2\,\Omega^{-1}\,mol^{-1}$, DMF): 45.5.

Complex **5**: Yield 81.4% (0.088 g). UV-Vis (λ_{max} nm, $\epsilon \times 10^4$ $(mol\,L^{-1})^{-1}\,cm^{-1}$): 260 (3.86), 377 (2.34). IR (KBr): 3403, 3206, 1655, 1591, 1558, 1098, 1468, 1328, 1022, 964, 839, 724, 643, 533, 451. MS (ESI-TOP, DMF) *m/z*: 293.2, 649.9, 651.3, 652.0, 652.9, 1298.1, 1299.7, 1300.6, 1302.1, 1302.6, 1304.2, 1305.3. Anal. Calcd for $C_{32}H_{28}N_{10}O_{14}Eu_2$ (%): C, 35.57; H, 2.61; N, 12.96; Eu, 28.13. Found: C, 35.66; H, 2.60; N, 12.84; Eu, 28.28. Λm ($cm^2\,\Omega^{-1}\,mol^{-1}$, DMF): 49.0.

Complex **6**: Yield 84.9% (0.093 g). UV-Vis (λ_{max} nm, $\epsilon \times 10^4$ $(mol\,L^{-1})^{-1}\,cm^{-1}$): 261 (5.13), 363 (3.23), 399 (3.18). IR (KBr): 3383, 3212, 1655, 1591, 1559, 1098, 1467, 1323,

1034, 964, 839, 727, 633, 535, 447. MS (ESI-TOP, DMF) *m/z*: 293.1, 651.1, 652.1, 653.2, 654.1, 655.5, 656.6, 657.8, 658.6, 659.1, 1300.0, 1301.4, 1302.5, 1303.7, 1305.4, 1306.9, 1310.1, 1313.3, 1315.0, 1315.9, 1317.2, 1319.0. Anal. Calcd for $C_{32}H_{28}N_{10}O_{14}Gd_2$ (%): C, 35.22; H, 2.59; N, 12.84; Gd, 28.82. Found: C, 35.37; H, 2.57; N, 12.73; Gd, 28.99. Λm ($cm^2\ \Omega^{-1}mol^{-1}$, DMF): 48.6.

Complex **7**: Yield 89.1% (0.098 g). UV-Vis (λ_{max} nm, $\epsilon \times 10^4$ $(mol\,L^{-1})^{-1}cm^{-1}$): 262 (4.49), 368 (2.75), 402 (2.81). IR (KBr): 3382, 3214, 1656, 1591, 1561, 1098, 1467, 1323, 1034, 965, 839, 728, 636, 535, 447. MS (ESI-TOP, DMF) *m/z*: 293.1, 654.9, 656.1, 657.3, 657.9, 658.7, 659.4, 660.3, 660.8, 661.3, 662.2, 663.0, 663.5, 664.2, 1315.2, 1316.9, 1317.8, 1324.4, 1325.6, 1328.6. Anal. Calcd for $C_{32}H_{28}N_{10}O_{14}Dy_2$ (%): C, 34.89; H, 2.56; N, 12.71; Dy, 29.50. Found: C, 34.74; H, 2.55; N, 12.62; Dy, 29.66. Λm ($cm^2\ \Omega^{-1}mol^{-1}$, DMF): 44.3.

Complex **8**: Yield 88.2% (0.098 g). UV-Vis (λ_{max} nm, $\epsilon \times 10^4$ $(mol\,L^{-1})^{-1}cm^{-1}$): 262 (5.03), 363 (3.07), 405 (3.25). IR (KBr): 3376, 3214, 1655, 1591, 1561, 1098, 1467, 1321, 1037, 961, 839, 729, 634, 536, 449. MS (ESI-TOP, DMF) *m/z*: 293.2, 663.1, 663.8, 664.3, 664.9, 665.3, 1326.2, 1327.6, 1328.2, 1328.9, 1329.5. Anal. Calcd for $C_{32}H_{28}N_{10}O_{14}Ho_2$ (%): C, 34.74; H, 2.55; N, 12.66; Ho, 29.81. Found: C, 34.62; H, 2.54; N, 12.78; Ho, 29.92. Λm ($cm^2\ \Omega^{-1}mol^{-1}$, DMF): 41.3.

Complex **9**: Yield 83.9% (0.093 g). UV-Vis (λ_{max} nm, $\epsilon \times 10^4$ $(mol\,L^{-1})^{-1}cm^{-1}$): 262 (4.93), 362 (2.90), 408 (3.13). IR (KBr): 3384, 3216, 1656, 1590, 1562, 1099, 1468, 1321, 1035, 963, 839, 729, 632, 535, 447. MS (ESI-TOP, DMF) *m/z*: 293.2, 660.1, 660.7, 661.7, 662.2, 663.1, 663.8, 664.4, 665.1, 665.9, 666.7, 667.5, 669.1, 669.9, 1320.1, 1320.7, 1321.8, 1323.4, 1324.2, 1326.5, 1327.9, 1329.0, 1329.5, 1330.2, 1331.0, 1331.8, 1334.1, 1335.0, 1336.1, 1338.3, 1339.6. Anal. Calcd for $C_{32}H_{28}N_{10}O_{14}Er_2$ (%): C, 34.59; H, 2.54; N, 12.61; Er, 30.11. Found: C, 34.48; H, 2.55; N, 12.72; Er, 30.24. Λm ($cm^2\ \Omega^{-1}mol^{-1}$, DMF): 37.1.

Complex **10**: Yield 86.1% (0.097 g). UV-Vis (λ_{max} nm, $\epsilon \times 10^4$ $(mol\,L^{-1})^{-1}cm^{-1}$): 262 (4.68), 363 (2.93), 406 (3.19). IR (KBr): 3400, 3213, 1656, 1591, 1562, 1100, 1469, 1324, 1034, 966, 839, 730, 635, 535, 450. MS (ESI-TOP, DMF) *m/z*: 293.1, 667.3, 669.2, 671.1, 671.9, 672.9, 674.3, 675.7, 1338.6, 1341.5, 1347.0, 1348.3, 1350.5, 1351.0. Anal. Calcd for $C_{32}H_{28}N_{10}O_{14}Yb_2$ (%): C, 34.23; H, 2.51; N, 12.48; Yb, 30.83. Found: C, 34.29; H, 2.50; N, 12.57; Yb, 30.69. Λm ($cm^2\,\Omega^{-1}mol^{-1}$, DMF): 39.4.

3. Results and discussion

3.1. *Syntheses of compounds*

8-Hydroxyquinoline-7-carbaldehyde-(isonicotinyl)hydrazone (**1**, H_2L) was prepared from equivalent molar amounts of 8-hydroxyquinoline-7-carbaldehyde and isonicotinylhydrazine (scheme 1). The lanthanide(III) complexes (**2**–**10**) were prepared from **1** and equivalent molar amounts of $Ln(NO_3)_3 \cdot 6H_2O$ (Ln = La^{3+}, Nd^{3+}, Sm^{3+}, Eu^{3+}, Gd^{3+}, Dy^{3+}, Ho^{3+}, Er^{3+}, Yb^{3+}), respectively. All the Ln(III) complexes are yellow powders, stable in air, soluble in DMF and DMSO, and slightly soluble in methanol, ethanol, acetonitrile, ethyl acetate, acetone, THF, and $CHCl_3$. Elemental analyses

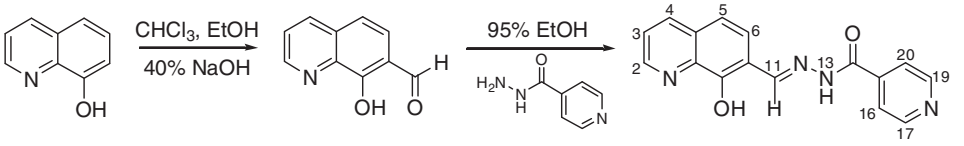

Scheme 1. The synthetic route for **1** (H_2L).

indicate that all these complexes are 1 : 1 metal to ligand and molar conductances in DMF indicate that all are non-electrolytes [38].

3.2. *Structures of Ln(III) complexes*

Comparison of IR bands between ligand and Ln(III) complexes: (1) Bands at $3403-3369_{br}$ assigned to ν(OH) of H_2O, $966-961_w$ assigned to ρ_r (H_2O), and $643-631_w$ assigned to ρ_w (H_2O) indicate that coordinated water is present in the Ln(III) complexes [35, 39]. (2) Bands at 1100–1095 assigned to ν(C–OM) which are similar to μ-O, especially at the lower frequencies, compared with complexes derived from 8-hydroxyquinoline-2-carbaldehyde with aroylhydrazines, indicate that binding of every metal to ligand takes place through a μ-O (M–O–M) linkage [20, 40]. (3) Bands at 1642_s assigned to ν(CO) and 3335_{vs} assigned to ν(NH) of isonicotinylhydrazine side chain of **1** disappear, indicating that they participate in the Ln(III) complexes with OC–NH– probably enolizing and deprotonating into $^-$O–CN–. (4) Band at 1568 assigned to ν(CN) of azomethine of **1** disappears and bands at 1562–1555 assigned to ν(CN) of pyridines of quinolinato units of Ln(III) complexes shift by 9–4 cm^{-1} in comparison with **1** indicate that both nitrogen atoms participate in the Ln(III) complexes. However, bands at 1591–1590 assigned to ν(CN) of pyridines of isonicotinylhydrazine units of Ln(III) complexes hardly shift in comparison with **1**. (5) Bands at $536-533_w$ assigned to ν(MO) and $451-436_w$ assigned to ν(MN) further indicate that oxygen and nitrogen participate in complexes. (6) All the Ln(III) complexes show bands at 1469–1465 (ν_1), 1328–1318 (ν_4), 1046–1031 (ν_2), 840–839 (ν_3), 730–7121 (ν_5), and $\Delta\nu(\nu_1-\nu_4) = 147 - 140\,cm^{-1}$, indicating that bidentate nitrate participate in the Ln(III) complexes [20, 21].

The results of elemental analyses, molar conductance, IR spectra, and ESI-MS data indicate that **1** is dibasic tetradentate, binding to Ln(III) through the phenolate oxygen, nitrogen of quinolinate, CN and $^-$O–CN– (enolized and deprotonated from OC–NH–) of the isonicotinylhydrazine side chain. Dimerization of this monomeric unit may occur through the phenolate oxygen atoms leading to a central four-membered $(LnO)_2$-ring. Radii of lanthanide(III) ions decrease gradually and the total difference of radii is only 14 pm from La^{3+} to Lu^{3+}; it is presumed that the metal complexes are structurally similar with binuclear compositions $[LnL(NO_3)(H_2O)_2]_2$ (figure 1). However, the m/z data (DMF solution) of complexes indicate that coordinated water of every powdered Ln(III) complex can be replaced by DMF molecules when dissolved in DMF solution, and that the composition of binuclear complex in DMF solution is $[LnL(NO_3)(DMF)_2]_2$. Additionally, the m/z peaks of $[H_2L + H]^+$, $[M/2]^+$, $[M/2 + H]^+$, $[M]^+$, $[M + H]^+$ and the isotope patterns of metal ions can be found

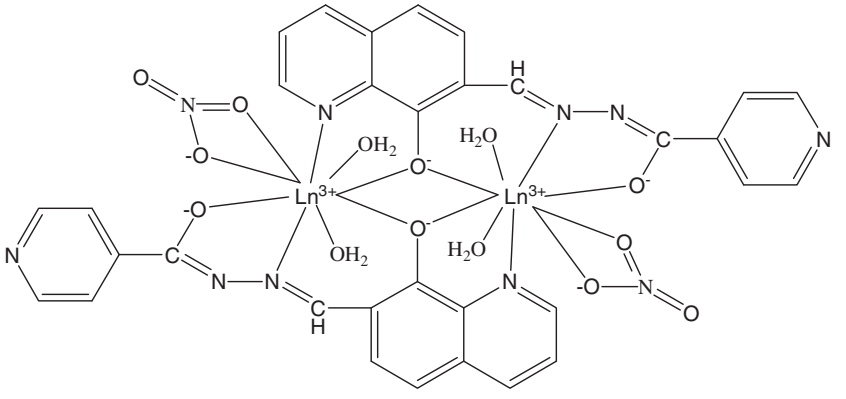

Figure 1. The suggested structure of binuclear Ln(III) complexes.

(see Supplementary material, figure S1), indicating that the binuclear complex exists as well as monomeric unit in DMF solution [41].

3.3. *Viscosity titration measurements*

Viscosity titration measurements were carried out to clarify the interaction modes between the investigated compounds and ct-DNA. Hydrodynamic measurements that are sensitive to length change of DNA (i.e., viscosity and sedimentation) are most critical criteria for binding modes in solution in the absence of crystallographic structural data, as viscosity is proportional to L^3 for rod-like DNA of length L [26, 42]. Intercalation involves the insertion of a planar molecule between DNA base pairs, resulting in a decrease in the DNA helical twist and lengthening of the DNA, therefore intercalators cause the unwinding and lengthening of DNA helix as base pairs become separated to accommodate the binding compound [26, 43]. Agents bound to DNA through groove binding do not alter the relative viscosity of DNA, and agents bound to DNA through electrostatic binding bend or kink the DNA helix, reducing its effective length and its viscosity concomitantly [33, 44]. With the ratio of the investigated compound to DNA (bps) increasing, the relative viscosity of DNA increases steadily (figure S2), indicating that intercalation takes place between the compounds and DNA helix. The increase in relative viscosity of DNA by every complex is more than by ligand, indicating more unwinding and lengthening of the DNA helix and higher affinity of complex binding to DNA than that of ligand.

3.4. *UV-Vis spectroscopic study*

The UV-Vis absorption spectra of the investigated compounds in the absence and presence of the ct-DNA were obtained in DMF : Tris-HCl buffer (5 mmol L^{-1}, pH 7.20) containing 50 mmol L^{-1} NaCl of 1 : 100 solutions, respectively. The UV-Vis spectra of H_2L have absorptions at 246 nm ($\epsilon = 2.17 \times 10^4$ $(\text{mol L}^{-1})^{-1}\text{cm}^{-1}$) and 353 nm ($\epsilon = 1.57 \times 10^4$ $(\text{mol L}^{-1})^{-1}\text{cm}^{-1}$), while the UV-Vis spectra of Ln(III) complexes present three bands at 248–262 nm ($\epsilon = 3.86$–5.13×10^4 $(\text{mol L}^{-1})^{-1}\text{cm}^{-1}$),

Table 1. K_b, K_{SV}, FC_{50}, SC_{50} ($OH^{\bullet}$ and $O_2^{-\bullet}$) for H_2L and Ln(III) complexes.

Compound	$K_b \times 10^5$ $(mol\,L^{-1})^{-1}$	$K_{SV} \times 10^5$ $(mol\,L^{-1})^{-1}$	FC_{50} ($\mu mol\,L^{-1}$) ($C_{compound}/C_{DNA,\ nucleotides}$)	SC_{50} ($\mu mol\,L^{-1}$) for $OH^{\bullet}$	SC_{50} ($\mu mol\,L^{-1}$) for $O_2^{-\bullet}$
1	6.94 ± 0.01	0.208 ± 0.001	45.82 (11.45)	143 ± 3	179 ± 5
2	9.5 ± 0.1	1.50 ± 0.04	7.191 (1.798)	4.365 ± 0.006	12.2 ± 0.8
3	10.6 ± 0.1	1.29 ± 0.03	8.497 (2.124)	3.45 ± 0.05	15 ± 3
4	11.1 ± 0.2	1.18 ± 0.03	8.894 (2.223)	2.3 ± 0.2	28 ± 5
5	17 ± 1	1.51 ± 0.04	7.684 (1.921)	8.8 ± 0.7	11.4 ± 0.8
6	12 ± 1	1.70 ± 0.02	6.333 (1.583)	13 ± 1	9.4 ± 0.7
7	16.7 ± 0.1	1.09 ± 0.02	8.356 (2.089)	8.2 ± 0.5	4.5 ± 0.1
8	10.5 ± 0.1	1.40 ± 0.02	7.377 (1.844)	4.99 ± 0.05	9.5 ± 0.5
9	12.2 ± 0.1	1.00 ± 0.01	9.232 (2.308)	3.64 ± 0.06	6.24 ± 0.07
10	10.2 ± 0.1	1.02 ± 0.02	8.867 (2.217)	5.3 ± 0.1	16 ± 2

377−356 nm ($\epsilon = 2.34-3.52 \times 10^4$ $(mol\,L^{-1})^{-1}\,cm^{-1}$), and 393−408 nm ($\epsilon = 2.38-3.25 \times 10^4$ $(mol\,L^{-1})^{-1}\,cm^{-1}$), which can be assigned to π–π^* transition of aromatic rings, π–π^* of conjugated aromatic rings and the charge transfer from ligand to metal ions ($L \rightarrow Ln^{3+}$), respectively [35, 39]. Isosbestic points at 453 nm for ligand and at 453−485 nm for Ln(III) complexes indicate that equilibria take place between compounds and DNA. Upon successive addition of ct-DNA (bps), the UV-Vis absorption of ligand shows a progressive hypochromism of 67.4% at 246 nm and 68.1% at 353 nm by approximately saturated titration end point at $C_{DNA} : C_{ligand} = 1.8 : 1$. Similarly, UV-Vis bands of complexes show progressive hypochromism of 13.8−63.6% at 248−262 nm and another progressive hypochromism of 14.3−53.4% at 377−356 nm by $C_{DNA} : C_{complex} = 1.0-1.6 : 1$. The obvious hypochromism indicates non-covalent intercalative binding of compound to the DNA helix, due to strong stacking interaction between the aromatic chromophore of the compound and base pairs of DNA [45, 46]. The magnitude of hypochromism is parallel to the intercalative strength and the affinity of a compound binding to DNA [42]. Figures S3 and S4 show plots of the UV-Vis titration and the plots of $[DNA]/(\epsilon_f - \epsilon_a)$ *versus* [DNA] for ligand and Ln(III) complexes, respectively. The binding constants ($K_b = 6.973$–17.09×10^5 $(mol\,L^{-1})^{-1}$) between DNA and the investigated compounds were determined and the values of K_b are listed in table 1. The value of K_b of EB (classical intercalative agent) binding to DNA investigated with the same conditions is 0.3068×10^5 $(mol\,L^{-1})^{-1}$ (figure S3). Figure 2 shows the plot of K_b with 4f electron number of metal ions. It is obvious that all the Ln(III) complexes have higher binding abilities to DNA than either ligand or EB; Eu(III) and Dy(III) complexes have much higher binding abilities to DNA. These Ln(III) complexes have stronger binding to ct-DNA *via* intercalation than those derived from 3-carbaldehyde chromone with isonicotinyl hydrazine and 1-phenyl-3-methyl-4-formyl-2-pyrazolin-5-one (PMFP) with isonicotinyl hydrazine, in which $K_b = 2.46$–7.6×10^5 $(mol\,L^{-1})^{-1}$ and $Ln = La^{3+}$, Nd^{3+}, Sm^{3+}, and Yb^{3+} [47, 48]. However, the Sm(III) complex derived from 8-hydroxyquinoline-7-carbaldehyde-(isonicotinyl)hydrazone shows weaker binding to ct-DNA *via* intercalation than that of Sm(III) complex derived from Congo red (CR) binding to herring sperm DNA, in which the K_b of $Sm(III)(CR)_3$ complex is 6.25×10^6 $(mol\,L^{-1})^{-1}$ at 18°C and 1.11×10^7 $(mol\,L^{-1})^{-1}$ at 26°C [49].

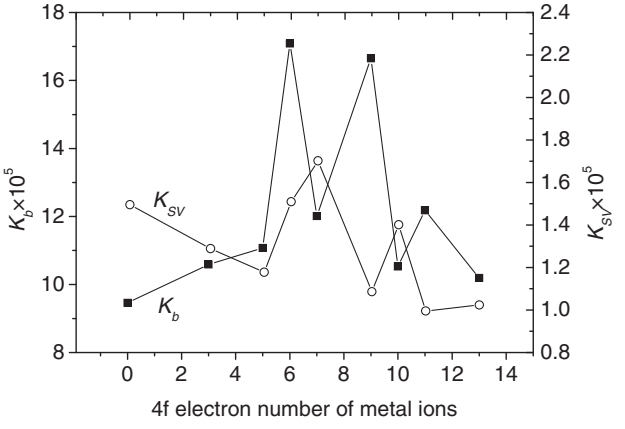

Figure 2. Plots of K_b and K_{SV} with 4f electron number of metal ions.

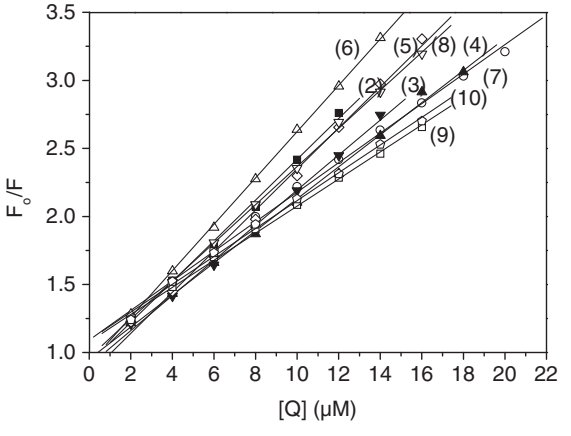

Figure 3. The Stern–Volmer plots for ligand and Ln(III) complexes in EB-DNA systems. $\lambda_{ex} = 525$ nm, $\lambda_{em} = 587$ nm, 298 K. The concentration of DNA is 4.0 μmol L^{-1} (nucleotides) and the concentration of EB is 0.32 μmol L^{-1}.

3.5. *DNA-EB quenching assay*

The fluorescence emission intensity of DNA-EB system decreased dramatically upon increasing amounts of either ligand or Ln(III) complexes, as shown in figure 3 and table 1, the values of K_{SV} are $0.2080-1.702 \times 10^5$ $(\text{mol L}^{-1})^{-1}$ for ligand and Ln(III) complexes. The Stern–Volmer quenching constant can be interpreted as the association or binding constant of the complexation reaction [26, 33, 50]. The loss of fluorescence intensity at the maximum wavelength indicates that most of the EB molecules have been displaced from EB-DNA complex and that the intercalative binding takes place between the investigated compound and DNA. The data of K_{SV} present a Gd(III) hump and the order that is not consistent with those of K_b determined by UV-Vis titration, indicating that the interaction mechanism is determined not only by complex formation

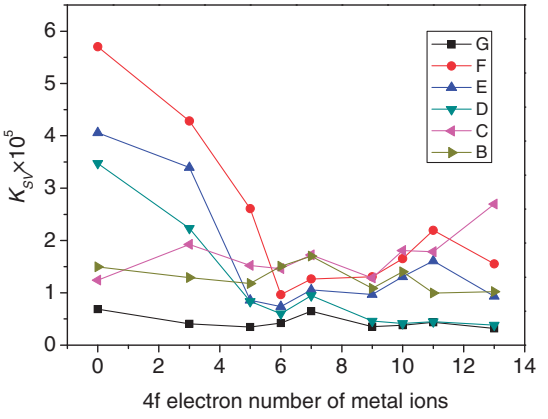

Figure 4. Plots of K_{SV} with 4f electron number of metal ions for Ln(III) complexes of Schiff bases B, C, D, E, F, and G.

but also by some weak interactions [30]. DNA intercalators have been used extensively as antitumor, antineoplastic, antimalarial, antibiotic, and antifungal agents [26]. There is a criterion for screening out antitumor drugs from others by the DNA-EB fluorescent tracer method, i.e., a compound may be used as a potential antitumor drug if it causes a 50% loss of DNA-EB fluorescence intensity by fluorescent titration before the molar concentration ratio of the compound to DNA (nucleotides) does not exceed 100 : 1 [51]. FC_{50} is introduced to denote the molar concentration of a compound that causes 50% loss in the fluorescence intensity of the EB-DNA system. According to the data of FC_{50} and the molar ratios of compounds to DNA (table 1), for FC_{50}, all the molar concentration ratios of the investigated compounds to DNA (1.583–11.45 : 1) are under 100 : 1, indicating that all these investigated compounds could be used as potential antitumor drugs and the antitumor activities of Ln(III) complexes may be better than that of ligand. However, their pharmacodynamical, pharmacological, and toxicological properties should be further studied *in vivo*. Figure 4 shows the plots of K_{SV} with 4f electron number of metal ions for Ln(III) complexes of Schiff bases 8-hydroxyquinoline-7-carbaldehyde-(isonicotinyl)hydrazone (B), 8-hydroxyquinoline-7-carbaldehyde-(benzoyl)hydrazone (C), 8-hydroxyquinoline-2-carbaldehyde-(benzoyl)hydrazone (D), 8-hydroxyquinoline-2-carbaldehyde-(*o*-hydroxybenzoyl)hydrazone (E), 8-hydroxyquinoline-2-carbaldehyde-(*p*-hydroxybenzoyl)hydrazone (F), and 8-hydroxyquinoline-2-carbaldehyde-(isonicotinyl)hydrazone (G). From this we can note that: (1) Ln(III) complexes of ligand C have higher binding abilities to DNA than those of ligand B; (2) the light rare-earth metal complexes of ligand D, E, and F present higher binding abilities to DNA, especially for La(III) and Nd(III) complexes; (3) every plot of K_{SV} has a slight Gd(III) hump, which may be related to the $4f^7$ electron effect.

3.6. *Scavenging activities for $HO^{\bullet}$ and $O_2^{-\bullet}$*

As shown in table 1, values of SC_{50} of ligand and Ln(III) complexes for $HO^{\bullet}$ are 143.1 and 2.344–13.33 μmol L^{-1}, respectively. Scavenging effects of Ln(III) complexes for

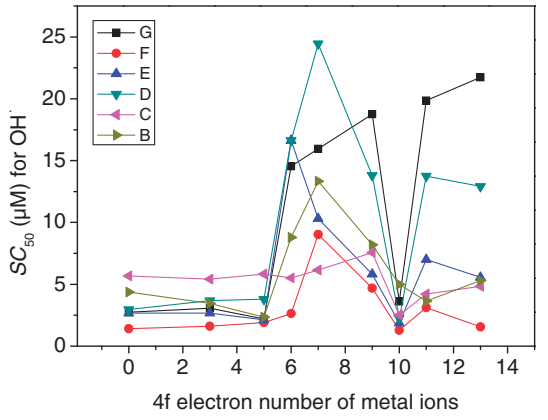

Figure 5. Plots of SC_{50} (μmol L^{-1}) of Ln(III) complexes of Schiff bases B, C, D, E, F, and G for $OH^{\bullet}$ with 4f electron number of metal ions.

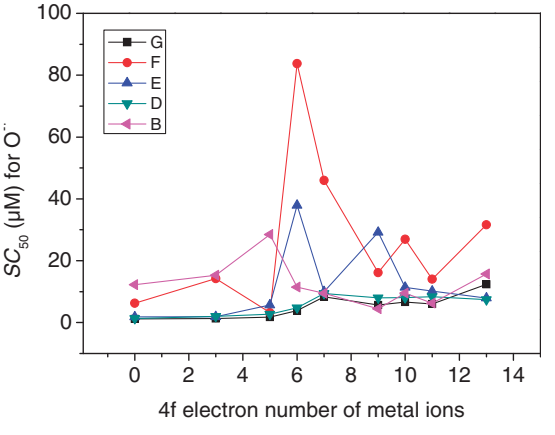

Figure 6. Plots of SC_{50} (μmol L^{-1}) of Ln(III) complexes of Schiff bases B, D, E, F, and G for $O_2^{-\bullet}$ with 4f electron number of metal ions.

$HO^{\bullet}$ are much higher than that of ligand, possibly in that the conjugated metal complexes can react with $HO^{\bullet}$ to form larger stable macromolecular radicals by typical H-abstraction reaction [52]. Additionally, values of SC_{50} of ligand and Ln(III) complexes for $O_2^{-\bullet}$ are 178.9 and 4.459–28.48 μmol L^{-1}, respectively. Scavenging effects of Ln(III) complexes and ligand for both $HO^{\bullet}$ and $O_2^{-\bullet}$ are much better than that of ascorbic acid (standard anti-oxidative agents for non-enzymatic reaction), whose value of SC_{50} for $HO^{\bullet}$ is 1.537 mg mL^{-1} (8.727 mmol L^{-1}) and the value of SC_{50} for $O_2^{-\bullet}$ is only 25% at 1.75 mg mL^{-1} (9.94 mmol L^{-1}) [53]. Figure 5 shows plots of SC_{50} (μmol L^{-1}) of Ln(III) complexes of Schiff bases B, C, D, E, F, and G for $OH^{\bullet}$ and figure 6 shows the plots of SC_{50} (μmol L^{-1}) of Ln(III) complexes of Schiff bases B, D, E, F, and G for $O_2^{-\bullet}$ with 4f electron number of metal ions, respectively. The conclusions are that: (1) La(III), Nd(III), Sm(III), and Ho(III) complexes and all the complexes of E

and F, especially complexes of F, have stronger scavenging abilities for $OH^{\bullet}$, however, the Eu(III) complexes of E and F have the lower scavenging abilities for $O_2^{-\bullet}$; (2) Eu(III), Gd(III), Dy(III), Er(III), and Yb(III) complexes have weaker scavenging abilities for $OH^{\bullet}$, especially complexes of D and G. However, almost all complexes of D and G have stronger scavenging abilities for $O_2^{-\bullet}$, especially complexes of G; (3) there are different mechanisms for scavenging $OH^{\bullet}$ and $O_2^{-\bullet}$. Furthermore, the scavenging abilities for $OH^{\bullet}$ and $O_2^{-\bullet}$ have no notable differences between these Ln(III) complexes and those derived from 3-carbaldehyde chromone with isonicotinyl hydrazine and PMFP with isonicotinyl hydrazine. Structurally, complex containing hydroxyl unit may increase the scavenging abilities for $OH^{\bullet}$, while complex containing *N*-heteroaromatic substituent shows stronger scavenging abilities for $O_2^{-\bullet}$.

Acknowledgments

This study was supported by China NNSF (20975046) and Gansu Educational Fund SRP (1010B-04).

References

[1] Y.B. Zeng, N. Yang, W.S. Liu, N. Tang. *J. Inorg. Biochem.*, **97**, 258 (2003).
[2] A.M. Pyle, T. Morii, J.K. Barton. *J. Am. Chem. Soc.*, **112**, 9432 (1990).
[3] J.K. Barton, J.M. Goldberg, C.V. Kumar, N.J. Turro. *J. Am. Chem. Soc.*, **108**, 2081 (1986).
[4] S. Mahadevan, M. Palaniandavar. *Inorg. Chim. Acta*, **254**, 291 (1997).
[5] S.J. Lippard. *Acc. Chem. Res.*, **11**, 211 (1978).
[6] S.M. Hecht. *Acc. Chem. Res.*, **19**, 383 (1986).
[7] D. Parker, R.S. Dickins, H. Puschmann, C. Crossland, J.A.K. Howard. *Chem. Rev.*, **102**, 1977 (2002).
[8] M. Albrecht, O. Osetska, R. Fröhliich. *Dalton Trans.*, 3757 (2005).
[9] R.B. Hunter, W. Walker. *Nature*, **178**, 47 (1956).
[10] D.M. Kramsch, A.J. Aspen, L.J. Rozler. *Science*, **213**, 1511 (1981).
[11] B.N. Ames, M.K. Shigenaga, T.M. Hagen. *PNAS*, **90**, 7915 (1993).
[12] A.A. Horton, S. Fairhurst. *Crit. Rev. Toxicol.*, **18**, 27 (1987).
[13] H.L. Wang, Z.Y. Yang, B.D. Wang. *Trans. Met. Chem.*, **31**, 470 (2006).
[14] S.Y. Chiang, J. Welch, F.J. Rauscher, T.A. Beerman. *Biochemistry*, **33**, 7033 (1994).
[15] J.M. Woynarowski, M. Mchugh, R.D. Sigmund, T.A. Beerman. *Mol. Pharmacol.*, **35**, 177 (1989).
[16] A.Y. Chen, C. Yu, B. Gatto, L.F. Liu. *PNAS.*, **90**, 8131 (1993).
[17] L.H. Schmidt. *Annu. Rev. Microbiol.*, **23**, 427 (1969).
[18] A.A. El-Asmy, A.Z. El-Sonbati, A.A. Ba-Issa, M. Mounir. *Trans. Met. Chem.*, **5**, 222 (1990).
[19] Y.C. Liu, Z.Y. Yang. *Biometals*, **22**, 733 (2009).
[20] Y.C. Liu, Z.Y. Yang. *J. Inorg. Biochem.*, **103**, 1014 (2009).
[21] Y.C. Liu, Z.Y. Yang. *J. Biochem.*, **147**, 381 (2010).
[22] Y.C. Liu, X.H. Jiang, Z.Y. Yang, X.D. Zheng, J.N. Liu, T.L. Zhou. *Appl. Spectrosc.*, **64**, 980 (2010).
[23] Y.C. Liu, Z.Y. Yang, K.J. Zhang, Y. Wu, J.H. Zhu, T.L. Zhou. *Aust. J. Chem.*, **64**, 345 (2011).
[24] Y.C. Liu, K.J. Zhang, Y. Wu, J.Y. Zhao, J.N. Liu. *Chem. Biodivers.* (in press), doi: 10.1002/cbdv.201100322.
[25] F. Zsila, Z. Bikádi, M. Simonyi. *Org. Biomol. Chem.*, **2**, 2902 (2004).
[26] D. Suh, J.B. Chaires. *Bioorg. Med. Chem.*, **3**, 723 (1995).
[27] S. Satyanarayana, J.C. Dabrowiak, J.B. Chaires. *Biochemistry*, **31**, 9319 (1992).
[28] A. Wolfe, G.H. Shimer Jr, T. Meehan. *Biochemistry*, **26**, 6392 (1987).
[29] P.X. Xi, Z.H. Xu, X.H. Liu, F.J. Cheng, Z.Z. Zeng. *Spectrochim. Acta, Part A*, **71**, 523 (2008).
[30] A. Ayar, B. Mercimek. *Process Biochem.*, **41**, 1553 (2006).
[31] C.C. Winterbourn. *Biochem. J.*, **182**, 625 (1979).
[32] C.C. Winterbourn. *Biochem. J.*, **198**, 125 (1981).

[33] B.D. Wang, Z.Y. Yang, P. Crewdson, D.Q. Wang. *J. Inorg. Biochem.*, **101**, 1492 (2007).
[34] Z.Y. Guo, R.E. Xing, S. Liu, H.H. Yu, P.B. Wang, C.P. Li, P.C. Li. *Bioorg. Med. Chem. Lett.*, **15**, 4600 (2005).
[35] T.M.A. Ismail. *J. Coord. Chem.*, **58**, 141 (2005).
[36] H. Chomatsu, H. Yasuo, I. Tetsuya. *Nippon Kagaku Zasshi*, **77**, 1107 (1956).
[37] R.X. Lei, J. Cheng, Y.Y. Jia, C.F. Liu, Y.C. Liu. *J. Baoji Univ. Arts Sci.*, **28**, 206 (2010) (in Chinese).
[38] W.J. Geary. *Coord. Chem. Rev.*, **7**, 81 (1971).
[39] M.M. Moawad, W.G. Hanna. *J. Coord. Chem.*, **55**, 439 (2002).
[40] J.M. Ou-Yang. *Chinese J. Inorg. Chem.*, **13**, 315 (1997).
[41] M. Berglund, M.E. Wieser. *Pure Appl. Chem.*, **83**, 397 (2011).
[42] D.S. Sigman, A. Mazumder, D.M. Perrin. *Chem. Rev.*, **93**, 2295 (1993).
[43] R. Palchaudhuri, P.J. Hergenrother. *Curr. Opin. Biotech.*, **18**, 497 (2007).
[44] S. Satyanarayana, J.C. Dabrowiak, J.B. Chaires. *Biochemistry*, **31**, 9319 (1992).
[45] J.K. Barton, A.T. Danishefsky, J.M. Goldberg. *J. Am. Chem. Soc.*, **106**, 2172 (1984).
[46] H.L. Lu, J.J. Liang, Z.Z. Zeng, P.X. Xi, X.H. Liu, F.J. Chen, Z.H. Xu. *Trans. Met. Chem.*, **32**, 564 (2007).
[47] Y. Li, Z.Y. Yang. *J. Coord. Chem.*, **63**, 1960 (2010).
[48] M.F. Wang, Z.Y. Yang, Y. Li, H.G. Li. *J. Coord. Chem.*, **64**, 2974 (2011).
[49] H.Z. Pan, X.M. Wang, H.B. Li, Q. Yang, L.S. Ding. *J. Coord. Chem.*, **63**, 4347 (2010).
[50] L.A. Bagatolli, S.C. Kivatinitz, G.D. Fidelio. *J. Pharm. Sci.*, **85**, 1131 (1996).
[51] Z.L. Li, J.H. Chen, K.C. Zhang, M.L. Li, R.Q. Yu. *Sci. China Ser. B*, **21**, 1193 (1991).
[52] J.I. Ueda, N. Saito, Y. Shimazu, T. Ozawa. *Arch. Biochem. Biophys.*, **333**, 377 (1996).
[53] R. Xing, H. Yu, S. Liu, W. Zhang, Q. Zhang, Z. Li. *Bioorg. Med. Chem.*, **13**, 1387 (2005).